

Cite this article as: Chen Zhiyong, Xu Yingqiang, Li Miaoling, et al. Structural Design and Numerical Simulation Optimization of SiC Wood Ceramic Composite Armor[J]. Rare Metal Materials and Engineering, 2021, 50(04): 1146-1155.

Structural Design and Numerical Simulation Optimization of SiC Wood Ceramic Composite Armor

Chen Zhiyong^{1,2}, Xu Yingqiang¹, Li Miaoling², Li Bin², Xiao Li¹, Wu Zhenghai¹

¹ School of Mechanical Engineering, Northwestern Polytechnical University, Xi'an 710072, China; ² School of Mechanical Engineering, Luoyang Institute of Science and Technology, Luoyang 471023, China

Abstract: Based on the bulletproof mechanism of ceramic composite armor, structural design and numerical simulation optimization of SiC/UHMWPE fiber composite armor were carried out to satisfy the protection requirements of vehicle. Penetration depth of bullet was taken as the evaluation standard, and the thickness, shape, size, and layout of SiC wood ceramic bullet proof sheet were considered as the research factors. An orthogonal simulation optimization scheme of four factors and three levels were designed, when the surface density of ceramic composite armor was 38 kg/m². Bulletproof performance was simulated by ANSYS/LS-DYNA finite element software. The optimized size parameters owing to the minimal penetration depth of bullet were selected. Accordingly, a SiC wood ceramic composite armor was prepared, and the bulletproof performance of designed ceramic composite armor was up to the protection standard of NATO AEP-55 STANAG 4569 level II as determined by the real bullet shooting test. Results show that the designed structure has 8 mm-thick SiC wood ceramic bulletproof panel and 13.7 mm-thick UHMWPE fiber bulletproof panel. The bulletproof panel is made of 4900 mm² hexagonal SiC wood ceramic bulletproof sheets. The influencing factors of SiC wood ceramic bulletproof sheet on the bulletproof performance is as follows: arrangement position>thickness>size>shape.

Key words: ceramic; bulletproof material; composite armor; finite element analysis; orthogonal design method

The research and production capacity of bulletproof materials reflect the military strength of a country and is an important guarantee for maintaining national and national security. The types of bulletproof materials are becoming more and more abundant, which are widely used in helicopter, bulletproof vehicle, etc. How to develop light, efficient, and inexpensive protective armor is a significant research topic in the field of military industry, aviation, and high-end vehicles in various countries^[1].

Bulletproof materials mainly include metals, ceramics, and fiber composite materials. Metals have a high material strength and toughness. When encountering high-speed impact penetration, metals have high plastic deformation ability and uniform deformation. However, metals have a high density and easy to rust; therefore, it is difficult to achieve a balance between reducing the weight and enhancing the protection performance. Ceramic has high hardness, modulus of elas-

ticity, and low density relative to metals, good chemical stability, high temperature resistance, erosion resistance, and wear resistance, which can well resist the erosion of high-speed armor piercing bullet by reducing armor mass. However, ceramic has the disadvantages of low fracture toughness, low thermal expansion coefficient, and poor resistance to multiple ballistic impacts. Therefore, it cannot be used alone for bulletproof armor. The characteristics of high-performance fiber are low density and elastic modulus, high strength, elongation, and corrosion resistance. Fiber composite bulletproof materials, mainly used in bulletproof clothes and bulletproof helmets and other bulletproof field, not only have light weight and good flexibility, but also can be designed with simple molding process^[2,3].

Simple materials cannot satisfy the upgrading requirements of lightweight and protective performance for bulletproof materials. Now, ceramic composite armor is composed

Received date: April 08, 2020

Foundation item: National Natural Science Foundation of China (51675427); Science and Technology Key Project of Henan Province of China (192102210026, 202102210074); Science Foundation of Henan International Joint Laboratory of Composite Cutting Tools and Precision Machining

Corresponding author: Xu Yingqiang, Ph. D., Professor, School of Mechanical Engineering, Northwestern Polytechnical University, Xi'an 710072, P. R. China, Tel: 0086-29-88460958, E-mail: xuyngqng@nwpu.edu.cn

Copyright © 2021, Northwest Institute for Nonferrous Metal Research. Published by Science Press. All rights reserved.

of a ceramic face plane and a fiber composite backplane. This composite material is lightweight, and has better bulletproof performance, design performance, and simple preparation process. In recent years, great developments have been made in theoretical research and application technology^[4,5].

Ceramic bulletproof materials are generally Al_2O_3 , SiC, and B_4C . Al_2O_3 is widely used as bulletproof materials because of its low cost, but has the lowest bulletproof grade and the largest density. B_4C has the best bulletproof performance and the least density, but is the most expensive. SiC wood ceramics are between the two; it is a new type of ceramic material made of wood with a biological structure and excellent properties by reaction sintering. Wood is renewable and has low cost and natural cellular structure. SiC ceramic has excellent properties such as high strength, good wear resistance, chemical corrosion, and thermal stability. SiC wood ceramics combines the advantages of two materials, its surface plane shows good bulletproof performance such as a high tensile strength to weight ratio, good mechanical properties, and low porosity content^[6].

Studies have been conducted on ceramic composite armor materials such as bulletproof mechanism, selection of material layer, structural design, material preparation, and numerical simulation of bulletproof performance. Ahmad et al^[7] studied the ballistic impact characterization of high-strength steels, namely, AISI 4340 and DIN 100Cr6, using 7.62 mm armor piercing (AP) projectiles and considering four hardness levels and five area densities. According to the results, the AISI 4340 steel with 50 HRC showed the best ballistic performance among the investigated materials. Sergio et al^[8] designed a multilayer composite armor with ceramic as the bulletproof panel and Curaua fiber as the first bulletproof back plate. The bulletproof performance was verified by impedance matching and SEM analysis. The results showed that Curaua composite can effectively absorb the residual energy after the bullet penetrates the ceramic debris. Sergio^[9] assessed the performance of multilayered armor systems (MAS), which was composed of a front $\text{Al}_2\text{O}_3\text{-Nb}_2\text{O}_5$ ceramic plate, followed by either aramid fabric layer or Curaua fiber reinforced polyester matrix composite layer, and backed with an aluminum alloy sheet. Ballistic impact tests were performed with 7.62 mm caliber ammunitions, and the efficacy of MAS as an armor component was confirmed. Fidan et al^[10] characterized single and repeated low velocity impact damage behavior of glass fiber reinforced polyester (GFRP) armor steel composite; CBCT was used to provide a novel, multiscale approach for assessing impact damage. Deformation areas of both single and repeatedly impacted GFRP armor steel composites were assessed three-dimensionally by CBCT.

Numerical simulation is an important analysis method to study the bulletproof performance of a composite armor. Andrea et al^[11] established a finite element analysis model of ceramic composite armor based on the Fourier transform and Wiener Hopf technology, studied the impact of bulletproof back plate stiffness on the brittle failure of bulletproof ceramic, and determined the stress intensity factor. Daniel et al^[12] studied a new ceramic composite armor made of Al_2O_3 plane

and UHMWPE, evaluated the configuration modeling method, simulated and analyzed the bulletproof performance, and ensured that the configuration model is correct by comparing the analysis result of V50. Zhang et al^[13] evaluated the effect of steel structure and glass fiber reinforced plastic structure on the perforation resistance of composite materials, carried out a series of high-speed ballistic impact tests on the ship's cabin wall armor system, and carried out numerical simulation on the ship's cabin wall composite armor system. The numerical results were consistent with the experimental results. Hu et al^[14] studied mosaic SiC ceramics with different geometries (cylindrical, hexagon, and square) spliced as the front layer on the back support plate of UHMWPE laminate and its ballistic performance through experiments under the penetration of an AP projectile. The results showed that the bulletproof property is enhanced with increasing the size of mosaic ceramics. Chen et al^[15] carried out a structural design and numerical simulation of mosaic ceramic composite armor, and target test was also conducted. The results showed that the numerical simulation method proposed in this study can better simulate the penetration of bullets into mosaic ceramic composite armor.

The literature review shows various research directions for bulletproof composite armor, but most of them are limited to qualitative analysis or quantitative test comparison. Quantitative analysis of the effect of SiC ceramic thickness, shape, size, and layout position on the bulletproof performance and evaluation of influencing trends are rarely involved in combining numerical simulation and real bullet shooting.

Based on excellent mechanical properties, bulletproof performance, high efficient utilization of SiC wood ceramic materials, and the protection requirements of light bulletproof vehicles, we designed a SiC wood ceramic composite armor bulletproof scheme in this study. ANSYS/LS-DYNA was used to carry out an orthogonal numerical simulation optimization design with four factors and three levels for the design scheme. SiC wood ceramic composite armor samples with the best design scheme were prepared and tested with real bullets. A method for preparing low-cost and high-performance SiC wood ceramic composite armor was explored, which provides a theoretical basis and research direction for the structural design of composite armor of SiC wood ceramic.

1 Bulletproof Scheme Design

The protection level is the basis for designing a bulletproof vehicle protection system, and it is also the primary problem to be solved in the study of a vehicle bulletproof scheme. This research used protection standards AEP-55 STANAG 4569 on level II of NATO, which used 7.62 mm×39 mm API to shoot the target plates at a velocity of 695 m/s, and the target plate was unaffected^[16].

1.1 Structural design

Ceramic has excellent properties, but suffers from some defects such as small molding size and poor plasticity. Therefore, it cannot be used for bulletproof materials independently, and must be supported by a backplane^[17,18]. To provide the full

advantages of ceramic bulletproof performance, the material of backplane should be able to resist the impact kinetic energy of bullets, and it should also have sufficient rigidity to support the ceramic material^[19]. Ceramic panel and backplane are adhered with a special rubber.

The bulletproof ceramic panel is spliced by some small ceramic tablets or a whole block. At present, whole ceramic panels can be produced in a large scale with high molding rate and good bulletproof homogeneity^[20]. However, this ceramic panel suffers from serious damage after impact, reducing the stiffness of whole ceramic panel. Depending on different shapes of the back plane, the whole ceramic panel needs different customized molds in difficult forming process, and the cost increases. In contrast, spliced ceramic panel has a good anti multiple attack ability, and different shapes can be quickly spliced depending on the backplane without a special customized mold. Therefore, the spliced ceramic panel was selected in the scheme^[21]. In addition, a crack arresting layer was added on the outer side of ceramic panel to enhance the protective effect, and the whole ceramic composite armor was attached to the automobile profile. A schematic diagram of ceramic composite armor is shown in Fig.1.

1.2 Material selection of bulletproof back plate

The main functions of backplane are to support the ceramic panel and to absorb the residual kinetic energy of bullets. If the supporting capacity of backplane is weak, the ceramic panel will be broken and splashed prematurely; the advantages of ceramic materials cannot be achieved. Therefore, the material of backplane should have a high stiffness and adhesive intensity with the ceramic panel, and then the ceramic material can provide excellent bulletproof performance^[22,23]. From the perspective of absorbing residual kinetic energy, the intensity of impact resistance of backplane material has a direct effect on bulletproof performance of composite armor. The backplane is required to withstand bullet impact force with adequate thickness and elastic modulus. Fiber reinforced plastic composites are the best choice for backplane material, which have light weight, high strength, good forming performance, and excellent ballistic performance. High-performance fibers used in composite materials are carbon fiber, glass fiber,

ultrahigh-molecular-weight polyethylene fiber (UHMWPE), and aramid fiber (KEVLAR). UHMWPE has the highest specific modulus and specific strength and good toughness and abrasion resistance; its bulletproof performance is about 25% higher than KEVLAR^[24,25]. Therefore, in this scheme, UHMWPE was used as the backplane material.

1.3 Determination of optimization parameters

In the structural design for SiC wood ceramic composite armor, the controllable factors are thickness, shape, size, and layout of SiC wood ceramic sheets.

According to the analysis of previous experimental results of bullet penetration into the target plate, when the thickness ratio of ceramic bulletproof panel and fiber bulletproof back plate is between 1:2 and 1:1, the corrosion resistance of target plate is better. In this study, the surface density of the composite armor does not exceed 38 kg/m², and the integral value range of the thickness of SiC wood ceramic sheet is 6~10 mm. There are three positions for SiC wood ceramic chip: bulletproof panel, bulletproof backplane, and intermediate interlayer (the thickness of UHMWPE fiber composite at the front and back is the same)^[26,27].

In terms of theory and technology, spliced ceramic tablets can be molded into various shapes as long as they can be properly spliced. The normal shapes of ceramic tablets are circular, square, and regular hexagon, as shown in Fig.2. However, the applied range of circular ceramic tablets is restricted because the spliced gap is too large. The straight splicing gap of square ceramic tablets affects the bulletproof performance. However, the molding is simple, and the gap can be eliminated through offset arrangement. Regular hexagon ceramic pieces can be arranged tightly^[28]. To facilitate a comparison of the

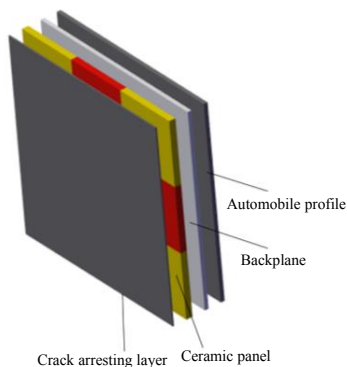


Fig.1 Schematic diagram of ceramic composite armor

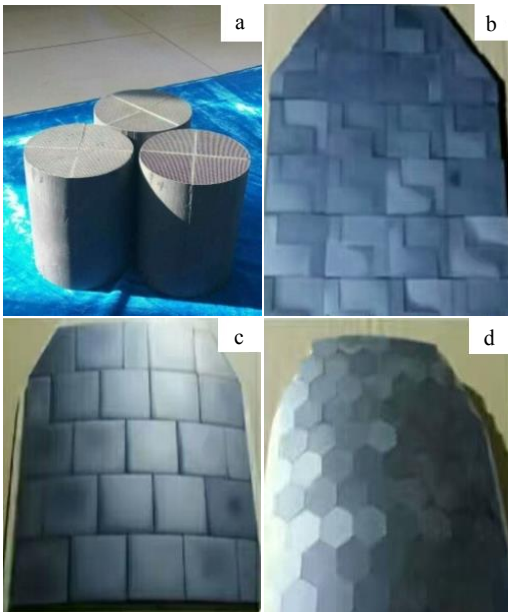


Fig.2 Various shapes of silicon carbide ceramics: (a) circular ceramic; (b) irregular ceramic; (c) square ceramic; (d) regular hexagon ceramic

performance, regular triangle, regular quadrilateral, and regular hexagon ceramic chips were selected in this study.

L9 (3⁴), namely, four factors and three levels, was selected as the numerical simulation optimization scheme to carry out orthogonal optimization design. The values of orthogonal factors in the simulation calculation are shown in Table 1, and orthogonal design scheme of numerical simulation is shown in Table 2.

2 Numerical Simulation

ANSYS/LS-DYNA was used to simulate the penetration of bullet into target plate, to study the trend of velocity and displacement with time when bullet penetrates a composite armor, to analyze the damage degree of ceramic composite armor, and to compare the effect of thickness, shape, size, and location of ceramic pieces on bulletproof performance to optimize the bulletproof scheme.

2.1 Geometric model

In Table 1, the ballistic performance of nine combina-

tions of target plates is simulated and analyzed. The bullet dimension is 7.62 mm×37.8 mm; target plate dimension is 300 mm×250 mm×20 mm. Other geometric parameters are shown in Table 1.

To make the analysis result more specific and realistic, all the central positions of four target plates are located on a whole ceramic tablet, and the bullet shot is perpendicular to the center of the target plate. To reduce the calculations, considering the symmetry of geometry shape and material behavior of bullet and target plate, 1/4 of target plate and bullet was built as a geometry model during the penetration, as shown in Fig.3.

2.2 Finite element model

The bullet and target plates were meshed using solid 8 node185 in software ANSYS. The finite element model is shown in Fig.4. As the bullet impact force, the mesh of target center area is dense and other areas are relatively sparse^[29].

During the numerical simulation analysis, the target plate was kept around displacement constraint, the bullet was load-

Table 1 Orthogonal factors in simulation analysis

Level	Factor			
	Thickness of ceramic sheet (A)/mm	Shape of ceramic sheet (B)	Size of ceramic sheet (C)/mm ²	Position of ceramic sheet (D)
1	6	Regular triangle	4900	Bulletproof panel
2	8	Regular quadrilateral	3600	Bulletproof backplane
3	10	Regular hexagon	2500	Bulletproof interlayer

Table 2 Orthogonal design scheme of simulation calculation

Project No.	Thickness of ceramic sheet (A)/mm	Shape of ceramic sheet (B)	Size of ceramic sheet (C)/mm ²	Position of ceramic sheet (D)
1	1	1	1	1
2	1	2	2	2
3	1	3	3	3
4	2	1	2	3
5	2	2	3	1
6	2	3	1	2
7	3	1	3	2
8	3	2	1	3
9	3	3	2	1

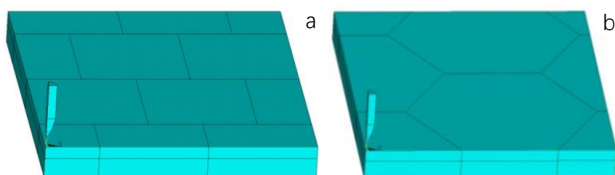


Fig.3 Geometry model during the penetration process (1/4 symmetrical structure): (a) quadrilateral ceramic plate and (b) regular hexagon ceramic plate

ed at a normal velocity of 695 m/s, contact among bullet, target plate, and adjoining ceramic tablets were defined, and the bullet and target plate adopted a single surface contact erosion algorithm. Bullet impacting target plate with a high velocity is a highly nonlinear problem. To reduce the computational complexity and improve the reliability of calculation, the calculation adopted point integration, but zero point integration easily causes the hourglass deformation and thus numerical oscillation. So, in this calculation, the standard algorithm was used to control the hourglass deformation, which introduces the viscous damping force of hourglass along the x_i direction at the node of each unit.

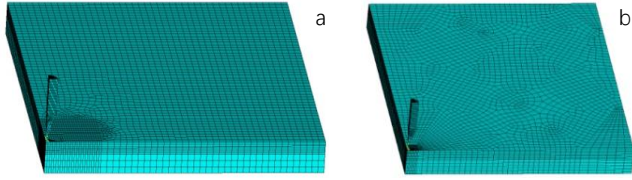


Fig.4 Finite element model during bullet penetration process (1/4 symmetrical structure): (a) quadrilateral ceramic plate; (b) regular hexagon ceramic plate

$$f_{ik} = -a_k \sum_{j=1}^4 h_{ij} \Gamma_{jk} h_{ij} = \sum_{k=1}^8 \dot{x}_i^k \Gamma_{jk} \quad (i=1,2,3; k=1,2,\dots,8) \quad (1)$$

where h_{ij} is model of hourglass modes, and negative indication means that the direction of hourglass damping component f_{ik} is opposite direction of hourglass modes.

$$a_k = Q_{kg} \rho V_c^{2/3} C/4 \quad (2)$$

where V_c is the volume of unit; C is sound velocity of material; Q_{kg} is defined constant, we get 0.1 in the calculation; ρ is density.

2.3 Material model

The bullet used Johnson-Cook material mode, the ceramic surface panel used JH-2 material mode, composite fiber backplane used Composite Damage Model material mode, and the state equation used Gruneisen mode^[30,31].

2.3.1 Material parameters of bullet

In Johnson-Cook material mode, yielding stress σ_y of the material is defined:

$$\sigma_y = (A + B\bar{\epsilon}^n)(1 + C \ln \dot{\epsilon}^*)(1 - T^{*m}) \quad (3)$$

where $\bar{\epsilon}^p$ is equivalent plastic strain; A , B , n , C and m are the constant of material, A is yielding stress, B and n are the effect of strain hardening.

General expression of fracture strain is:

$$\epsilon^f = (D_1 + D_2 \exp D_3 \sigma^*)(1 + D_4 \ln \dot{\epsilon}^*)(1 + D_5 T^*) \quad (4)$$

where σ^* is the ratio of dimensionless pressure to equivalent stress, $\sigma^* = p/\sigma_{\text{eff}}$ (p is average stress, σ_{eff} is Von Mises equivalent stress); D_1 , D_2 , D_3 , D_4 , D_5 are material yielding factors. The parameters of bullet material model are shown in Table 3.

2.3.2 Material parameters of wood ceramic panel

JH-2 constitutive equation is widely used for ceramic and other brittle materials. It can be expressed as follows:

$$\sigma' = (1 - D)\sigma'_i + D\sigma'_f \quad (5)$$

$$D = \sum \frac{\Delta \epsilon^p}{\epsilon_f^p} \quad (6)$$

$$p = \begin{cases} K_1 u + K_2 u^2 + K_3 u^3 & (u \geq 0) \\ K_1 u & (u < 0) \end{cases} \quad (7)$$

where σ'_i is Von-Mises equivalent stress of intact material, $\sigma'_i = A(p' + T')^n [1 + C \ln(\frac{\dot{\epsilon}}{\dot{\epsilon}_0})]$; σ'_f is Von-Mises equivalent stress of damage material, $[\sigma'_f = Bp'_M [1 + C \ln(\frac{\dot{\epsilon}}{\dot{\epsilon}_0})]$;

p' is pressure of dimensionless, and T' is maximum negative hydrostatic pressure of dimensionless; $u = \frac{\rho}{\rho_0} - 1$. The units

of Von-Mises stress σ' and pressure p' are Hugoniot equivalent yield stress of material σ_{HEL} and Hugoniot yield pressure p_{HEL} ; Damage D is defined as the ratio of the accumulative plastic strain and the failure strain $\epsilon_f^p = D_1(p' + T')^{D_2}$;

material parameters of silicon carbide ceramic model are shown in Table 4.

2.3.3 Material parameters of composite fiber backplane

The stress-strain constitutive relation of composite damage model with damage is expressed as

$$\begin{cases} \epsilon_1 = \frac{1}{E_1} (\sigma_1 - \nu_1 \sigma_2) \\ \epsilon_2 = \frac{1}{E_2} (\sigma_2 - \nu_2 \sigma_1) \\ \epsilon_3 = \frac{1}{E_3} (\sigma_3 - \nu_3 \sigma_1) \\ 2\epsilon_{12} = \frac{1}{G_{12}} \tau_{12} + \alpha \tau_{12}^3 \\ 2\epsilon_{13} = \frac{1}{G_{13}} \tau_{13} + \alpha \tau_{13}^3 \\ 2\epsilon_{23} = \frac{1}{G_{23}} \tau_{23} + \alpha \tau_{23}^3 \end{cases} \quad (8)$$

where ϵ_1 , ϵ_2 , ϵ_3 , ϵ_{12} , ϵ_{13} , ϵ_{23} are the longitudinal tensile strain, transverse tensile strain, normal direction tensile strain and the shear strain in the surface; σ_1 , σ_2 , σ_3 , τ_{12} , τ_{13} , τ_{23} are the longitudinal tensile stress, transverse tensile stress, normal direction tensile stress and the shear stress in the surface; ν_1, ν_2, ν_3 are the longitudinal, transverse and normal direction Poisson ratios, respectively; E_1 , E_2 , E_3 , G_{12} , G_{13} , G_{23} are the longitudinal tensile modulus, transverse tensile modulus, normal direction tensile modulus and the shear modulus in the surface; α is the nonlinear shear stress parameter.

In this model, Chang-Chang failure criterion is applied, which mainly contains fiber fracture failure criterion and compression damage failure criterion, and the fiber matrix interface bond ideal and mechanical performance parameters are calculated from the components and volume content of each composition^[32]. The parameters of UHMWPE fiber composite material model are shown in Table 5.

Table 3 Material parameter of bullet

$\rho_0/\text{kg}\cdot\text{m}^{-3}$	A/GPa	n	C	E/GPa	B	m	μ	σ_c/GPa	T_M/K	T_R/K
7890	1.7	0.12	0.016	200	0.2E9	1	0.3	0.9	2520	273
$C_V/\text{J}\cdot(\text{kg}\cdot\text{K})^{-1}$	p/GPa	D_1	D_2	D_3	D_4	D_5	$C_0/\text{m}\cdot\text{s}^{-1}$	S	γ_0	α
134	77	0.08	4.44	-3.12	0.004	0	4250	2	2.17	0

Table 4 Material parameters of SiC wood ceramics

$\rho_0/\text{kg}\cdot\text{m}^{-3}$	A	n	C	T/GPa	B	m	HEL/ GPa	$\sigma_{\text{HEL}}/\text{GPa}$
3090	0.96	0.65	0.0	0.426	0.35	1.0	150	130
$P_{\text{HEL}}/\text{GPa}$	G/GPa	K_1/GPa	K_2/Pa	K_3/Pa	β	D_1	D_2	$\sigma^*\text{fmax}$
5.9	180	210	0	0	1	0.48	0.48	1.0

Note: HEL is material strength limit

3 Numerical Simulation Results

When the bullet impacts the ceramic panel with a high speed, the bullet head deforms and produces a shock wave, which then attenuates the stress wave. The stress wave is reflected back after arriving the ceramic panel, and these stress waves which are superimposed over incident stress waves form free stress waves along the impact direction. These free stress waves can produce a grand stress that cracks the ceramic panel. As shown in Fig.5, stress waves spread rapidly and diffuse all around, causing the crack to develop into the surrounding area. However, the stress waves are limited by the boundaries of ceramic tablets. It restricts further expansion of ceramic cracks, and the ceramic tablet forms a fracture conical structure (Hertzian inverted cone)^[33].

The head of bullet becomes blunt, caused by crashing in the impact process, and the resistance increases further. After the kinetic energy decreases, the bullet continues to penetrate the fiber composite backplane. UHMWPE can still consume a lot of kinetic energy of bullet by the tensile failure. First of all, shear failure occurs, followed by a tensile failure, and then UHMWPE is delaminated, caused by fiber debonding and pulling out. A large circular deformation known as “back convex” is formed^[34]. Fig. 6 shows the numerical simulation results of bullet penetration.

Penetration depth, back convex and penetration rate are important indexes of bullet penetration capability and bulletproof performance of target plate. Penetration depth, which is the most important evaluation index, refers to the depth below the surface of the target plate after warhead impacts the target plate. In general, the three indicators are in direct proportion. The smaller the time interval between the residual velocity

and zero after the bullet is fired and penetrates the target plate, the smaller the penetration depth and back convex height of the bullet, indicating better bulletproof performance of the target plate^[35]. Therefore, the penetration depth of bullet is selected as the evaluation index of bulletproof performance of ceramic composite armor.

Numerical simulation was carried out according to the orthogonal conditions shown in Table 1, and the penetration depth of bullet was obtained. The results are shown in Table 6. Among the numerical simulation schemes, Scheme 9 ($\text{A}_3\text{B}_3\text{C}_2\text{D}_1$) has the lowest penetration depth. According to the R_j range analysis, the order of factors affecting the bulletproof performance is as follows: ceramic plate position>ceramic plate thickness>ceramic plate size>ceramic plate shape. The optimal order of ceramic thickness is 8 mm>10 mm>6 mm. The optimal order of ceramic plate position is as follows: bulletproof panel>bulletproof interlayer>bulletproof backplane. The optimal order of size is 4900 mm²>3600 mm²>2500 mm². The optimal order of shape is as follows: regular hexagon, regular quadrilateral, and regular triangle. The optimized design scheme shown in Table 6 is as follows: the thickness of ceramic sheet is 8 mm, the arrangement position of ceramic sheet is bulletproof panel, the size of ceramic sheet is 4900 mm², and the shape of ceramic sheet is regular hexagon.

According to the optimized design Scheme 10, the numerical simulation was carried out again. The penetration depth of the bullet is 16.0 mm, which is indeed the minimum penetration depth.

The velocity-time curve, displacement-time curve in penetration process in Scheme 10 are shown in Fig.7 and Fig.8, respectively. The penetration velocity of bullet approximately linearly decreases in the initial stage. With the progress of penetration, the bullet penetration resistance decreases caused by the broken ceramic. Therefore, the bullet penetration velocity slows down. When the bullet reaches the connect area between the ceramic panel and composite fiber backplane, the fibers further consume the kinetic energy of bullet, reducing the bullet velocity rapidly. As the fibers are broken down, the bullet velocity slows down to zero, and even the bullet is bounced back. It can form a relatively small velocity with op-

Table 5 Material parameters of UHMWPE

E_{11}/GPa	E_{22}/GPa	E_{33}/GPa	E_{12}/GPa	E_{13}/GPa	E_{23}/GPa	Poisson Ratio, μ
4.2	39	39	1.21	3.014	3.014	0.0314
$\rho_0/\text{kg}\cdot\text{m}^{-3}$	X_T/MPa	X_C/MPa	S_{12}/MPa	S_{13}/MPa	S_{23}/MPa	S_T/MPa
970	966	292	2.13	31.4	31.4	11.78

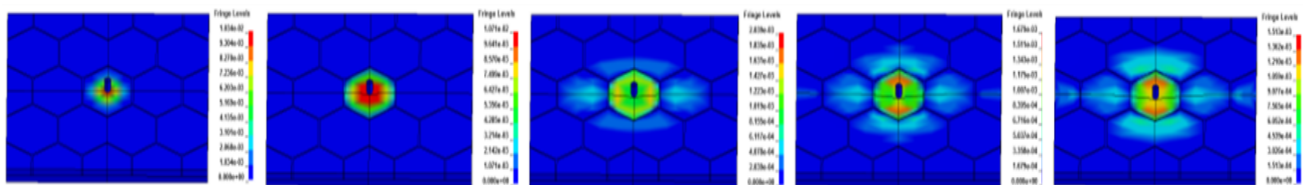


Fig.5 Stress transfer process of regular hexagon ceramic plane

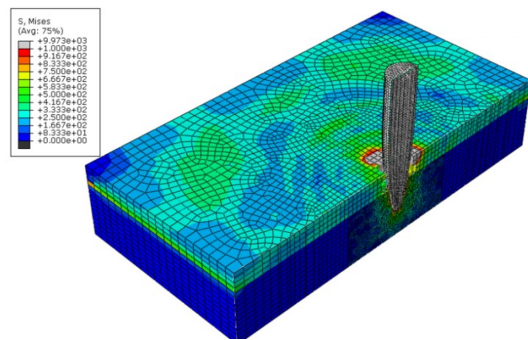


Fig.6 Numerical simulation results of bullet penetration process

posite direction of impacting.

4 Experimentation

4.1 Preparation and properties of SiC wood ceramics panel

SiC wood ceramics tablet is made from short carbon fiber powder and poplar powder by dry compression molding. Through liquid-phase silicon infiltration at a high temperature, 8 mm-thick SiC wood ceramics with a uniform structure and excellent mechanical properties were obtained. The main performance parameters of SiC wood ceramics tablet are shown in Table 7.

Fig.9 shows the SEM photographs of polished section of SiC wood ceramics. The bright white part is free silicon, and

Table 6 Orthogonal design of simulation calculation and simulation calculation results

Project No.	Thickness of ceramic sheet (A)/mm	Shape of ceramic sheet (B)	Size of ceramic sheet (C)/mm ²	Position of ceramic sheet (D)	Penetration depth/mm
1	6	Regular triangle	4900	Bulletproof panel	16.4
2	6	Regular quadrilateral	3600	Bulletproof backplane	17.5
3	6	Regular hexagon	2500	Bulletproof interlayer	17.2
4	8	Regular triangle	3600	Bulletproof interlayer	16.7
5	8	Regular quadrilateral	2500	Bulletproof panel	16.2
6	8	Regular hexagon	4900	Bulletproof backplane	16.7
7	10	Regular triangle	2500	Bulletproof backplane	17.6
8	10	Regular quadrilateral	4900	Bulletproof interlayer	16.7
9	10	Regular hexagon	3600	Bulletproof panel	16.1
k_1	17.03	16.90	16.6	16.23	
k_2	16.53	16.80	16.76	17.27	
k_3	16.80	16.67	17.00	16.87	
R_j	0.50	0.23	0.40	1.04	

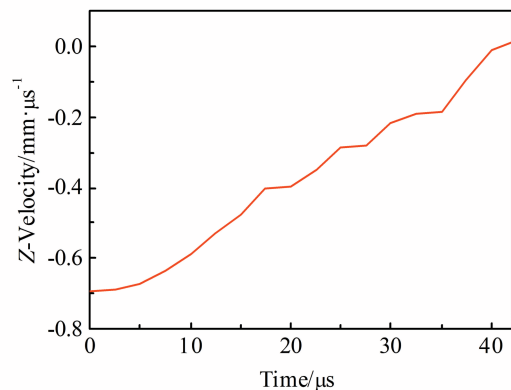


Fig.7 Velocity-time curve of the bullet in penetrating target plate process

the gray part is SiC. The black part is the gap. Fig.10 shows the microstructure of SiC wood ceramics. The bar structure is short cut carbon fiber.

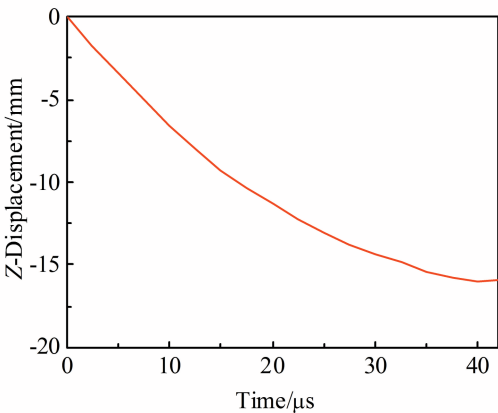


Fig.8 Displacement-curve of bullet in penetrating target plate process

4.2 Preparation and performance of the composite fiber backplane

In this experiment, 13.7 mm-thick UHMWPE fiber rein-

Table 7 Performance parameters of SiC wood ceramic sample

Density/kg·m ⁻³	Elasticity modulus/GPa	Vickers hardness, HV/×10 MPa	Bending strength/MPa	Fracture toughness/MPa·m ^{1/2}
3090	289	2630	426	3.1

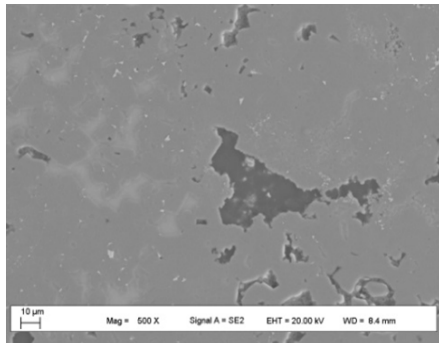


Fig.9 SEM image of SiC wood ceramics surface

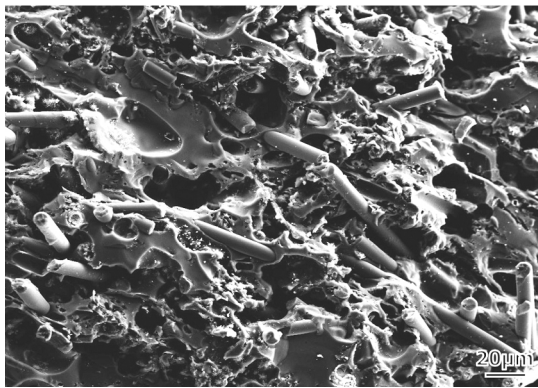


Fig.10 Microstructure of the SiC wood ceramics



Fig.11 UHMWPE backplane

Table 8 Performance parameters of UHMWPE backplane

Density/ kg·m ⁻³	Elasticity modulus/GPa	Tensile strength/ GPa	Extensibility/ %
970	101	3.1	5.3

forced resin backing material was prepared by hot pressing with UHMWPE fiber free cloth, as shown in Fig.11. The main performance parameters of UHMWPE backplane are shown in Table 8.

The SiC wood ceramic panel and the composite fiber back panel were bonded and cold pressed. To prevent the ceramic panel from bursting and splashing prematurely when it is penetrated by the warhead, a special adhesive was used to bond and cover the high-strength fabric on the outside of ceramic target plate as the crack arrest layer, and the ceramic target plate covered with the crack arrest layer is shown in Fig.12.

4.3 Ballistic test

The target test system consists of experimental guns, velocity measurement target plate, timer, backing material, etc. A schematic diagram is shown in Fig. 13. The experimental gun is a ballistic rifle. The distance between shooting platform and target plate is 30 m. The bullet uses API 7.62 mm steel bullet; three bullets are perpendicular to the target plate, the velocity is 695 m/s, as measured by a velocity measurement target plate^[36].

As shown in Fig.14, after shooting, the target plate panel and back plate are well bonded. The height and diameter of convexity are smaller, and the size distribution is more consistent. There is no large area of ceramic falling off at the impact point, and the ceramic cracks are radial.



Fig.12 Ceramic target plate covered with crack arrest layer

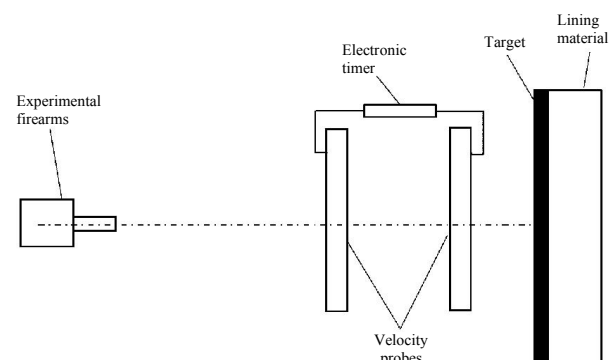


Fig.13 Schematic diagram of the target test system

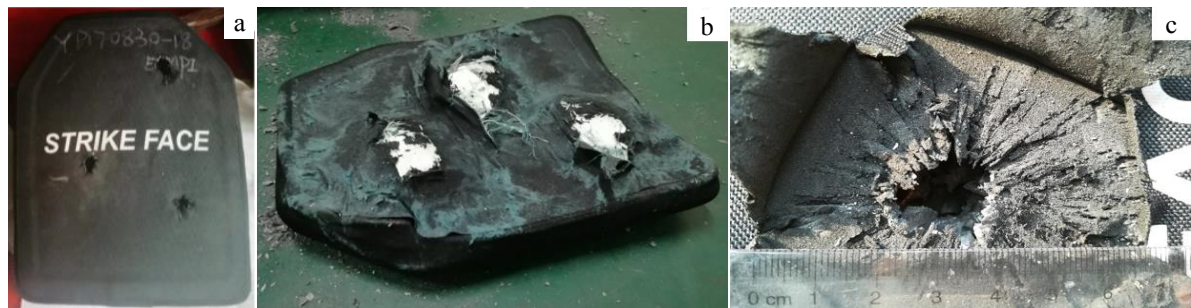


Fig.14 Target plate after bullet penetration: (a) panel, (b) back plate, and (c) crater shape

Table 9 Comparison between numerical simulation results and experimental results

Target plate No.	Shot condition	Simulated zero time of bullet/ μ s	Penetration depth/mm		Back convex height/mm	
			Simulation value	Test mean value	Simulation value	Test mean value
10	No penetration	41.8	16.0	17.3	14.2	15.8

The velocity-time curve, displacement-time curve, and deformation result of bullet in penetrating target plate process were combined, and the key indexes of numerical simulation results and test results are compared, as shown in Table 9.

5 Conclusions

1) According to an orthogonal simulation calculation scheme of four factors and three levels, the best structural form of the designed ceramic composite armor is determined. It consists of a 8 mm-thick SiC wood ceramic bulletproof panel and a 13.7 mm-thick UHMWPE fiber bulletproof panel. The bulletproof panel is made of a hexagonal SiC wood ceramic bulletproof panel with an area of 4900 mm².

2) The order of factors influencing the bulletproof performance is as follows: position of ceramic sheet>thickness of ceramic sheet>size of ceramic sheet>shape of ceramic sheet.

3) According to the optimized structural parameters, the penetration depth of bullet in numerical simulation scheme is 16.0 mm, which is the minimum penetration depth in orthogonal simulation schemes.

4) Gruneisen equation of state, Johnson-Cook constitutive model for bullet, JH-2 constitutive model for ceramic panel, and composite damage model for fiber back can be used to simulate the penetration process of bullet to ceramic composite armor.

5) The results of numerical simulation and real bullet shooting test show that the bulletproof performance of designed ceramic composite armor structure satisfies the requirements of NATO AEP-55 STANAG 4569 class II bulletproof standard, and wood ceramics has a good application prospect in the bulletproof field.

References

1 Wang Q X, Zhang H M, Cai H N et al. *Computational Materials Science*[J], 2017, 1129: 123

2 Jin J C, Wang C. *Applied Mechanics & Materials*[J], 2012,12: 2871
3 Gabrovsek S, Colwill I, Stipidis E. *The Journal of Defense Modeling and Simulation*[J], 2016, 13: 399
4 Jie Jiang, Xia Dong, Chen Meiyu et al. *Materials Herald*[J], 2013, 27: 70
5 Roberto M, Francois B. *Bioinspiration & Biomimetics*[J], 2016, 11: 1
6 Ma T, Yan Z L, Wang H et al. *Rare Metal Materials and Engineering*[J], 2011, 40(1): 215
7 Ahmad S, GovindG, Zhang Xianfeng et al. *International Journal of Impact Engineering*[J], 2017, 105: 54
8 Sergio N M, Fabio O B, Edio P L et al. *Polymer Engineering and Science*[J], 2016, 57: 947
9 Sergio N M, André B S F, Eduardo S L et al. *Materials Science Forum*[J], 2017, 7: 329
10 Fidan S, Bora M O, Coban O et al. *Plastics Engineers*[J], 2016, 37: 583
11 Andrea N, Enrico R. *Acta Mechanica*[J], 2016, 227: 159
12 Daniel B, Alfredo R F, Sérgio F A et al. *International Journal of Impact Engineering*[J], 2012, 43: 63
13 Zhang Yuanhao, Chen Changhe, Zhu Xi. *Chinese Journal of Ship Research*[J], 2017, 12: 53 (in Chinese)
14 Hu D A, Zhang Y M, Shen Z W et al. *Ceramics International* [J], 2017, 43: 10 368
15 Chen Zhiyong, Xu Yingqiang, Chen Guangwei et al. *Materials China*[J], 2019, 38(5): 497 (in Chinese)
16 Liu Sheng, Lv Panke, Zhang Yanpeng. *Ordinance Material Science and Engineering*[J], 2011, 34(6): 84 (in Chinese)
17 Liu Wei, Yang Jun. *Hot Working Technology*[J], 2011, 40: 108 (in Chinese)
18 Li Shutao, Zhong Tao, Miao Cheng et al. *Ordinance Material Science and Engineering*[J], 2014(1): 1 (in Chinese)
19 Santosa S P, Arifurrahman F, Hizzudin M et al. *Procedia Engi-*

- neering[J], 2017, 173: 495
- 20 Zhang X Q, Fan X Y, Yan C et al. *ACS Applied Materials Interfaces*[J], 2012, 4: 1543
- 21 Grujicic M, Bell W C, Pandurangan B et al. *Materials & Design*[J], 2012, 34: 808
- 22 Tasdemirci A, Tunusoglu G, Güden M. *International Journal of Impact Engineering*[J], 2012, 44: 1
- 23 Hou Hailiang, Zhu Xi, Li Wei. *Acta Armamentarii*[J], 2013, 34: 105 (in Chinese)
- 24 Pandya K S, Pothnis J R, Ravikumar G et al. *Materials & Design*[J], 2013, 44: 128
- 25 Lin C C, Lin J H, Chang C C. *Journal of Forensic Sciences*[J], 2011, 56(5): 1150
- 26 Tasdemirci A, Tunusoglu G, Güden M. *International Journal of Impact Engineering*[J], 2012, 44: 1
- 27 Zhang Xinjie. *Development and Application of Materials*[J], 2012, 27: 103 (in Chinese)
- 28 Hu D Q, Wang J R, Chen Z G et al. *Journal of Ballistics*[J], 2017, 29: 73
- 29 Krishnan K, Sockalingam S, Bansal S et al. *Composites: Part B* [J], 2010, 41: 583
- 30 Li Maohui, Huang Xiancong, Wang Lei et al. *Ordnance Material Science and Engineering*[J], 2011, 34(6): 99 (in Chinese)
- 31 Wang M, Qin Q, Wang T J. *Acta Mechanica*[J], 2017, 228: 3265
- 32 Kim H, Nam I. *Journal of Applied Polymer Science*[J], 2012, 123: 2733
- 33 Guo Y N, Sun Q, Wu L. *Applied Mechanics and Materials*[J], 2012, 10: 397
- 34 Kyner A, Dharmasena K, Williams K et al. *International Journal of Impact Engineering*[J], 2017, 108: 229
- 35 Tasdemirci A, Tunusoglu G, Güden M. *International Journal of Impact Engineering*[J], 2012, 44: 1
- 36 Hu Liping, Wang Heping, Wang Zhihui et al. *Journal of Projectiles, Rockets, Missiles and Guidance*[J], 2010, 30(5): 90 (in Chinese)

碳化硅木质陶瓷复合装甲结构设计及数值模拟优化

陈智勇^{1,2}, 徐颖强¹, 李妙玲², 李 彬², 肖 立¹, 吴正海¹

(1. 西北工业大学 机电学院, 陕西 西安 710072)

(2. 洛阳理工学院 机械工程学院, 河南 洛阳 471023)

摘 要: 根据车辆的防护要求, 以陶瓷复合装甲防弹机理为依据, 进行碳化硅木质陶瓷/UHMWPE 纤维复合装甲结构设计和数值模拟优化, 并制备碳化硅木质陶瓷复合装甲, 进行实弹打靶验证防弹性能。在确保陶瓷复合装甲面密度为 38 kg/m²的前提下, 以子弹侵彻深度为评价标准, 以碳化硅木质陶瓷防弹片的厚度、形状、尺寸和布置位置为研究因素, 设计了四因素三水平的正交模拟优化方案, 利用有限元软件 ANSYS/LS-DYNA 对所设计的复合装甲的防弹性能进行数值模拟, 并比对数值模拟结果与实弹打靶试验结果。结果表明, 针对北约 AEP-55 STANAG 4569 II 级防护标准, 所设计的陶瓷复合装甲最优化的结构形式为 8 mm 厚的碳化硅木质陶瓷防弹面板、13.7 mm 厚的 UHMWPE 纤维防弹背板, 防弹面板采用面积为 4900 mm² 的正六边形碳化硅木质陶瓷防弹片拼接而成; 碳化硅木质陶瓷防弹片对防弹性能的主次影响因素为: 布置位置 > 厚度 > 尺寸 > 形状。

关键词: 陶瓷; 防弹材料; 复合装甲; 有限元分析; 正交设计法

作者简介: 陈智勇, 男, 1984 年生, 博士, 讲师, 西北工业大学机电学院, 陕西 西安 710072, 电话: 029-88460958, E-mail: 1854@163.com